Supporting Information

Mesoporous Silica Nanoplates Facilitating Fast Li^+ Diffusion as Effective Polysulfide-trapping Materials for Lithium-Sulfur Batteries

*Xiao Xiang[a], Jing Yi Wu[a], Qing Xuan Shi[a], Qing Xia[a], Zhi Gang Xue[a], Xiao Lin Xie[a] and Yun Sheng Ye[a]**

Key Laboratory of Material Chemistry for Energy Conversion and Storage, Ministry of Education, School of Chemistry and Chemical Engineering, Huazhong University of Science and Technology, Wuhan 430074, China

*E-mail: ysye@hust.edu.cn

Electrochemical measurements

Linear sweep voltammetry (LSV) was carried out on an electrolyte-soaked separator sandwiched between Li metal and stainless steel with a scan rate of 10 mV s^{-1} on an AUTOLAB impedance analyzer.

The Li-ion diffusion coefficient was evaluated by a series cyclic voltammetry (CV) scans with various scan rates from 0.1 to 0.5 mV s^{-1} and calculated by the Randles-Sevcik equation as follows:

$$I_p = 2.69 \times 10^5 n^{3/2} A D_{Li^+}^{1/2} C_{Li^+} v^{1/2} \quad \text{(S1)}$$

Where I_p is the peak current, n is the number of electrons transferred in the reaction (n=2 for Li-S batteries), A is the electrode area, D_{Li^+} is the Li-ion diffusion coefficient, C_{Li^+} is the change in the concentration of Li-ion, and v is the scan rate. The set-up for CV tests are as follows: Upper vertex potential (V): 3.000, Lower vertex potential (V): 1.500, Stop potential (V): 2.950, Number of stop crossings: 10, Step potential (V): 0.00500.

Characterization

Thermogravimetric analysis (TGA) was performed on Q50. Samples were heated from 30 to 500 ^oC with a rate of 10 ^oC min^{-1} under nitrogen at 10 mL min^{-1} and kept for an hour at 500 ^oC, after that, heating was continued to 800 ^oC. The specific area was calculated from the adsorption data in the relative pressure interval from 0.04 to 0.2 using the Brunauer-Emmett-Teller (BET) method. UV-Visible spectra were measured by a Evolution 220, Thermo Scientific spectrophotometer. The stabilities and discharge-charge performances of the cells were tested with a programmable battery cycler (LAND Electronic Co. Ltd). The cyclic voltammogram data were collected with a Solartron at a scan rate of 0.01 to 0.05 mV s^{-1} in a voltage window of 2.6–1.7 V. The coating thickness was measured by a stylus profiler (DektakXT, Bruker). Electrochemical impedance spectroscopy plots were collected with a Solartron Impedance Analyzer. Morphological characterizations of MSiNP and SiNPs were collected by scanning

electron microscope (SEM, Hitachi S-4700), energy-dispersive X-ray spectroscopy (EDX) elemental mapping (FEI Nova NanoSEM450) and transmission electron microscope (TEM, JEOL JEM-1200CX-II). X-ray photoelectron spectroscopy (XPS) [ESCA 2000 (VG Microtech)] tests were using a monochromatized AlKa anode.

Caracterization of weittibility and retainability

The electrolyte uptake (*EU*) was calculated by soaking weighed pristine S-electrode and S-electrode coated with FSiNP and FMSiNP in the electrolyte at 30 ^{o}C for 1 h. The EU values were determined by:

$$EU\ (\%) = (W_S\text{-}W_I)/W_I \times 100\% \quad \text{(S2)}$$

Where W_I and W_S are the weight of the initial cathode and cathode after soaking in the electrolyte, respectively.

The electrolyte retention (*ER*) was determined by setting soaked cathodes in an oven at 30 ^{o}C for 0.2, 0.4 and 12 h. The *ER* values were calculated by:

$$ER\ (\%) = 100\% - (W_s\text{-}W_D)/W_S \times 100\% \quad \text{(S3)}$$

Where W_S is the cathode after soaking in the electrolyte; W_D is the weight of soaked cathode after deposition in an oven at 30 ^{o}C .

Table S1. The electrolyte uptakes (EUs) and retention of S-electrode coated with FSiNP, MSiNP, FMSiNP and prinstine S-electrode.

	PP	FSiNP	FMSiNP
EU (%)	46.3	46.2	50
ER (0.2 h %)	0.96	0.96	0.97
ER (0.4 h %)	0.94	0.94	0.96
ER (12 h %)	0.93	0.92	0.95

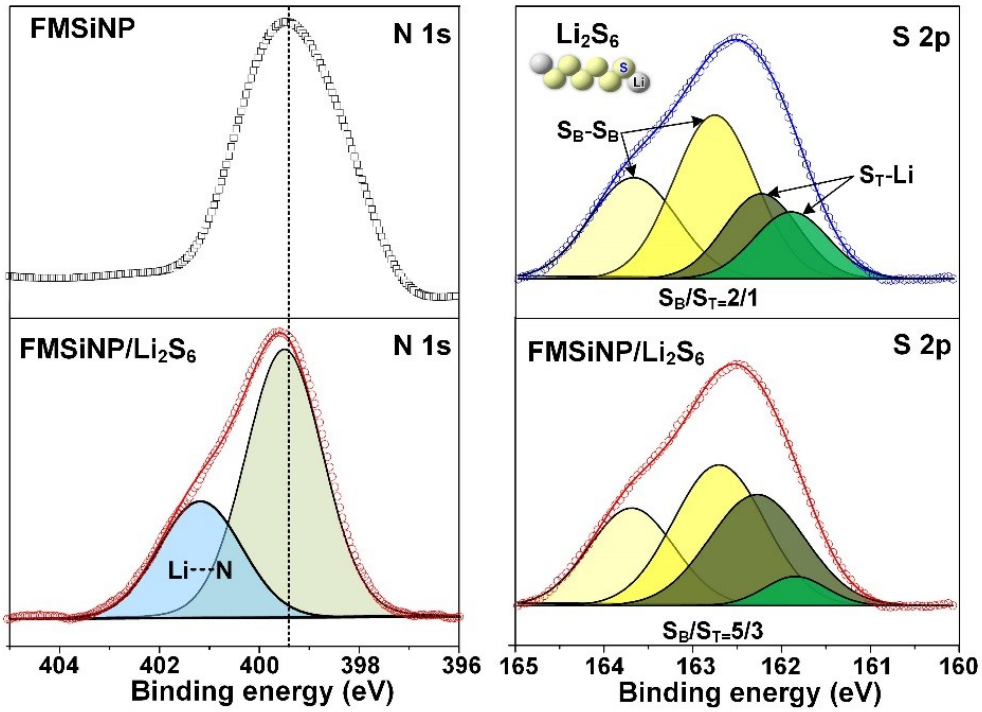

Figure S1. N 1s XPS spectra of (a) FMSiNP and (b) FMSiNP/Li_2S_6. S 2p XPS spectra of (c) Li_2S_6 and FMSiNP/Li_2S_6.

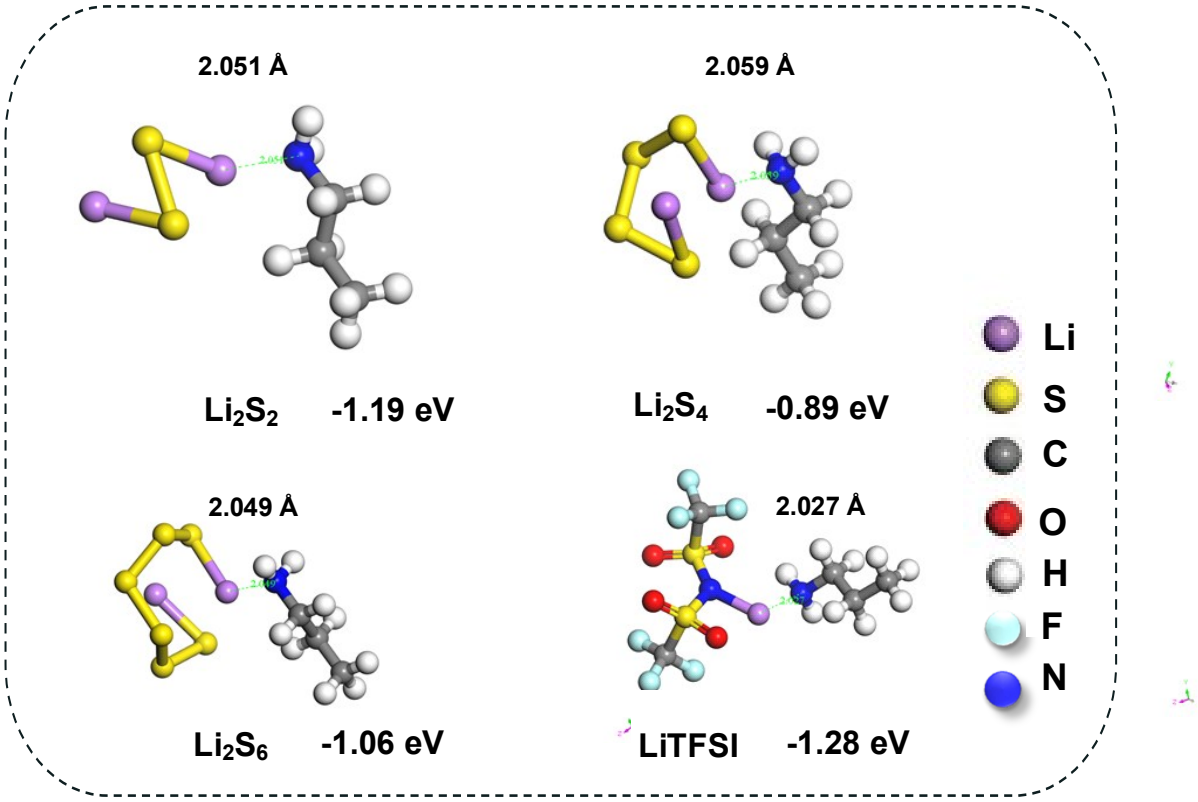

Figure S2. Molecular models of the interaction between FMSiNP and Li_2S_2, Li_2S_4, Li_2S_6 and LiTFSI by DFT calculations.

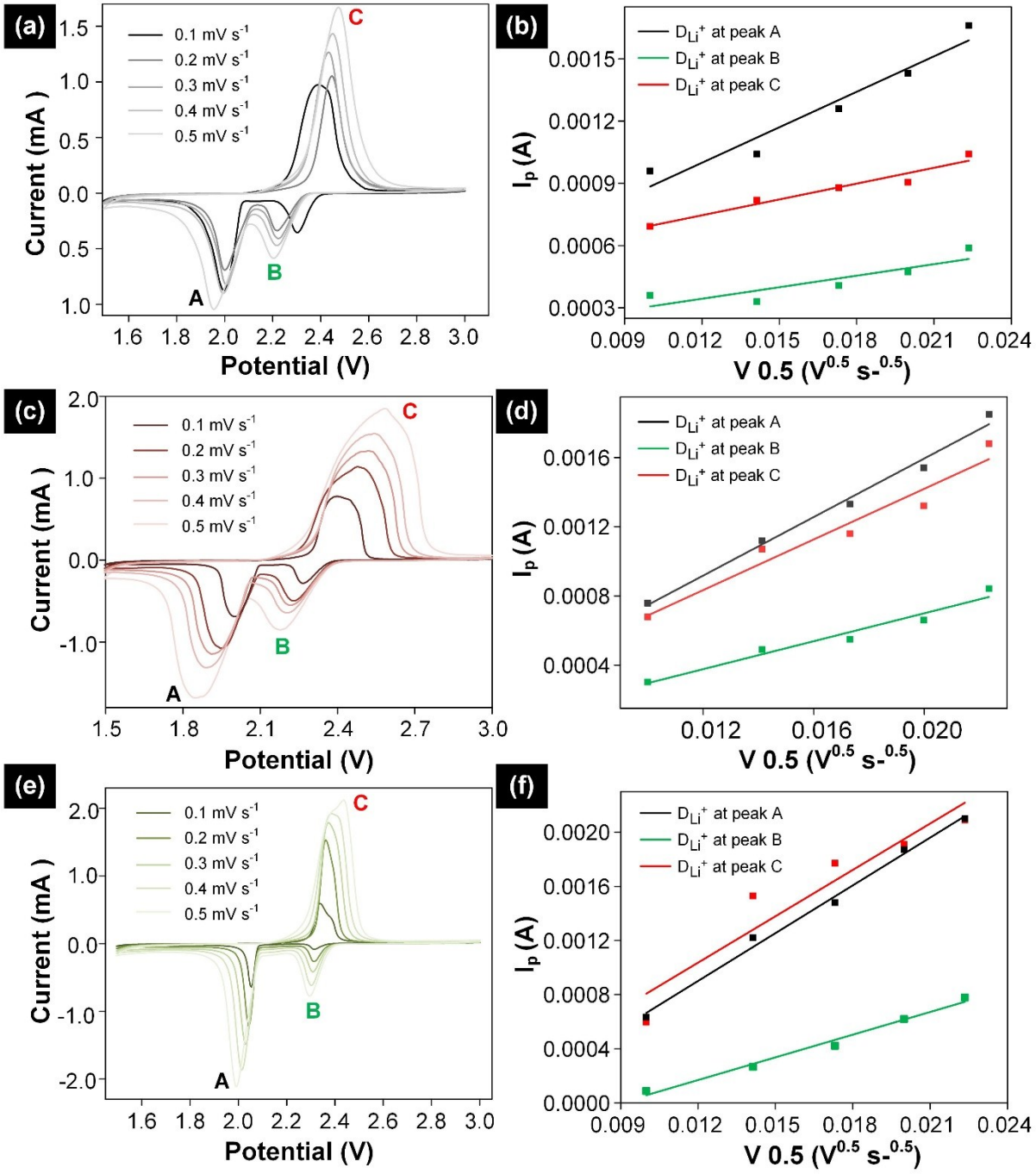

Figure S3. CVs at various scan rates and the linear fitting of the peak currents with the square root of the scan rates for the (a, b) Celgard separator, (c, d) FSiNP- and (e, f) FMSiNP-coated interlayers.

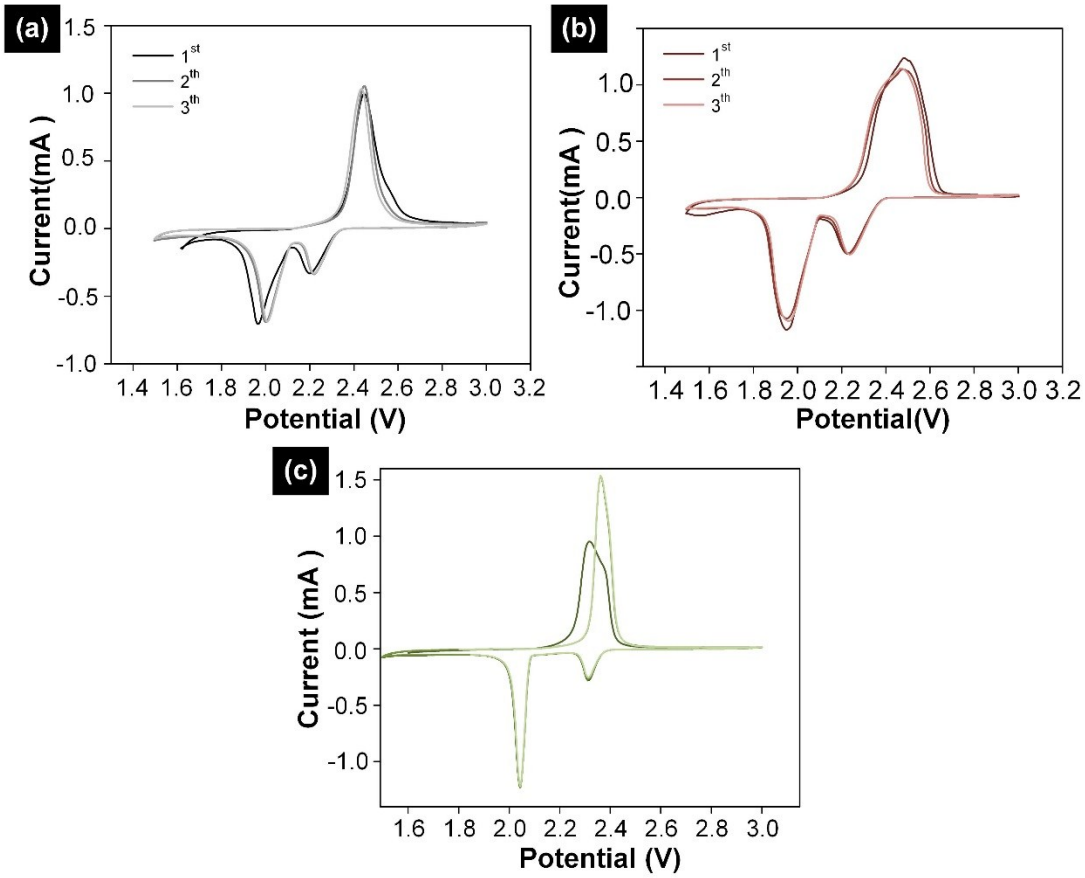

Figure S4. CV curves of (a) Celgard separator, (b) FSiNP- and (c) FMSiNP-coated interlayers swept in the voltage range of 1.3-3.2 V.

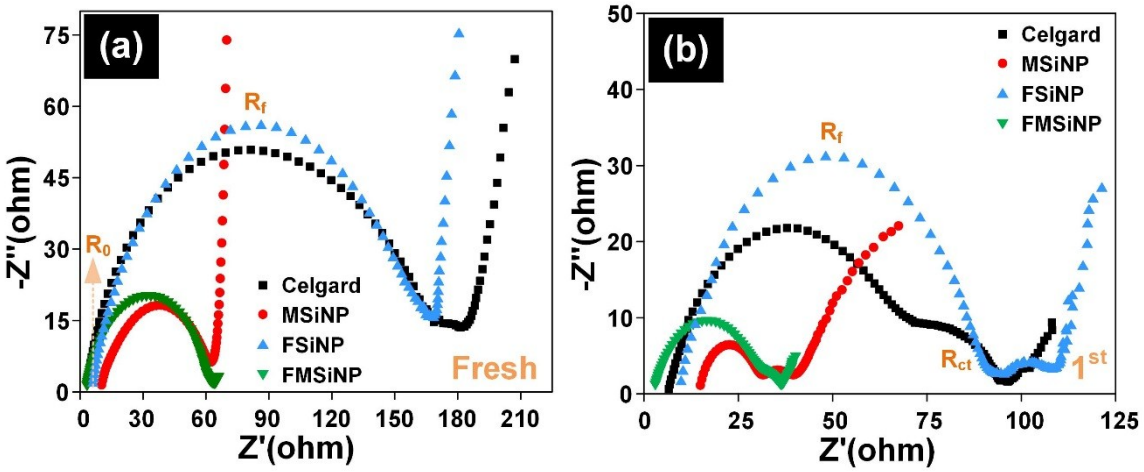

Figure S5. The Nyquist plots (a) the fresh cells without/with interlayers at a current of 0.5 C and (b) the cells after 10 cycles.

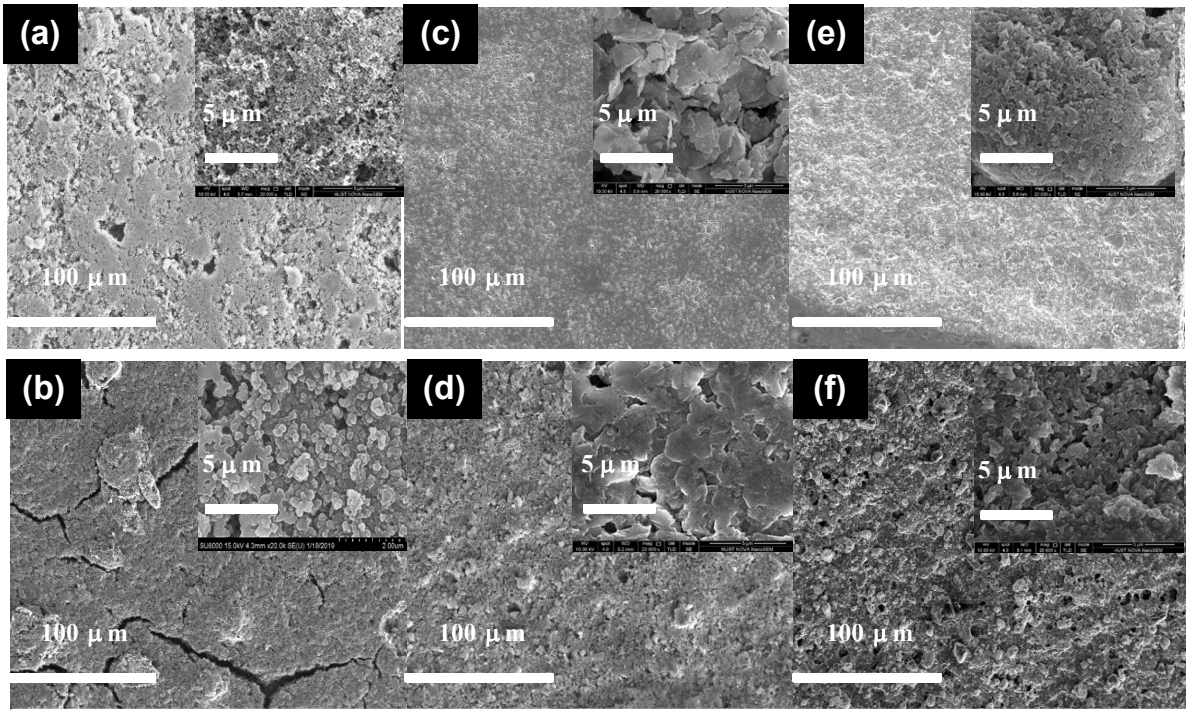

Figure S6. SEM images of (a) pristine S-electrode, S-electrode with (c) FSiNP and (e) FMSiNP before cycling; SEM images of (b) pristine S-electrode, S-electrode with (d) FSiNP and (f) FMSiNP after 100 cycles.

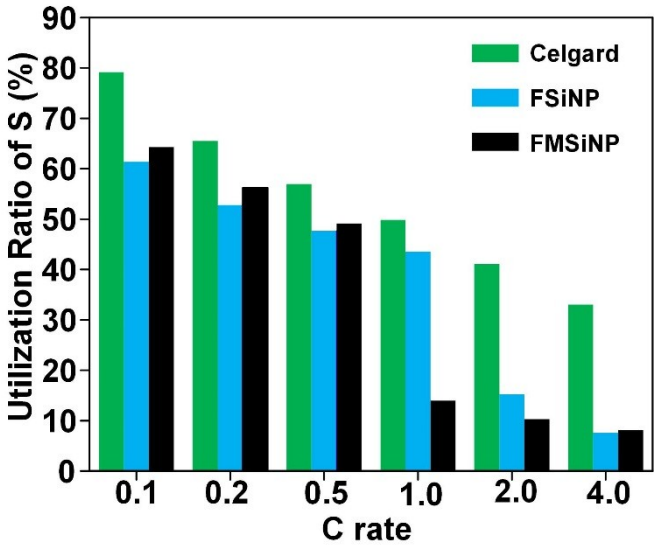

Figure S7. Utilization of the active materials of the cells without/with interlayers at various current ranges from 0.1 to 4.0 C.

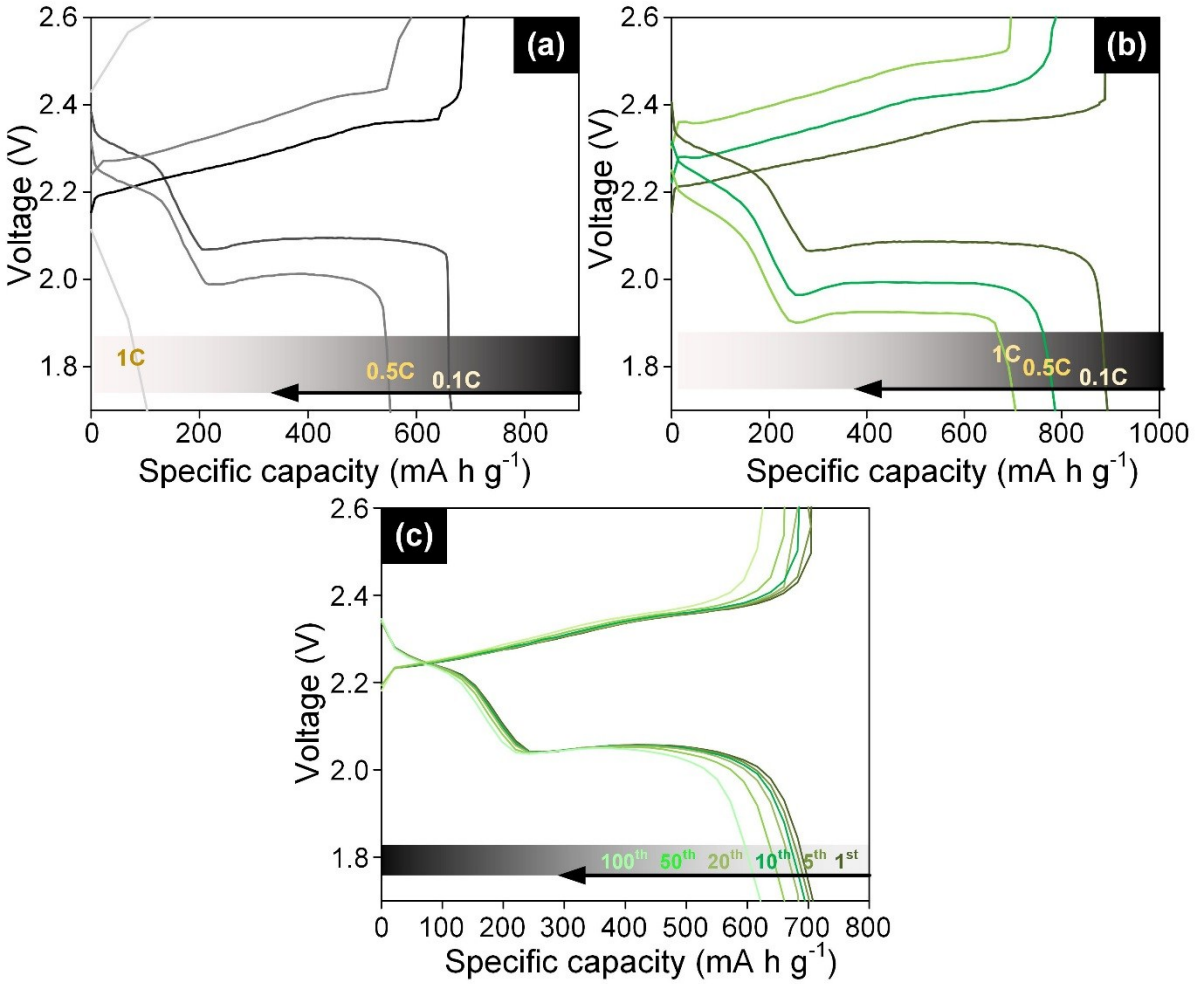

Figure S8. Discharge-charge profiles of (a) the pristine high-S loading cell and cells with (b) FMSiNP interlayer at various current ranges from 0.1 to 1.0 C; (c) Discharge-charge profiles of the high-S loading cell with FMSiNP interlayer at a rate of 1.0 C.

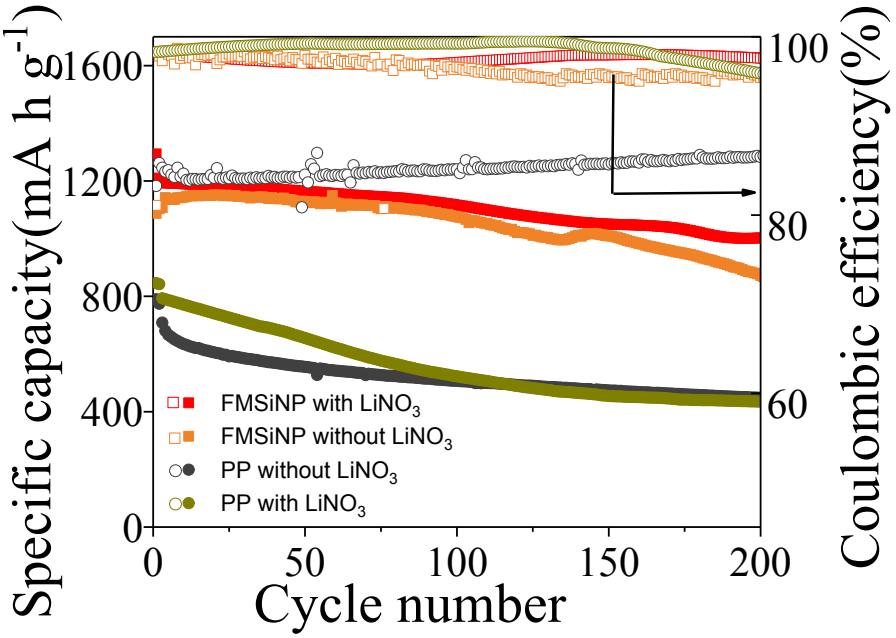

Figure S9. Electrochemical performance of the cells with/without FMSiNP interlayer using the electrolyte with/without $LiNO_3$ additive at a rate of 0.5 C.

Table S2. Performance comparison of the functional separators/or interlayers in recent publications.

Materials	Preparation method	Function	Electrochemical performance (initial capacity and degradation rate)	Cathode composition(sulfur content andareal loading)	Ref.
SRGO	Vacuum fltration	Electrostatic Repulsive Interaction	1300 mAh g^{-1} at 0.5C 0.15 % for 250 cycles	Ketjen Black/S 50 wt.%/1.3 mg cm^{-2}	S1
MCNF	Electrospinning	physicaly polysulfde-anchor	1549 mA h g^{-1} at 0.5C 0.17 % for 100 cycles	Pure sulfur 60 wt.%/1.4 mg cm^{-2}	S2
PANI-GO	Resting	Chemical interaction	1261 mA h g^{-1} at 0.5C 0.18 % for 150 cycles	Ketjen Black/S 49 wt.%/1.96 mg cm^{-1}	S3
PEDOT:PSS	Spraying	Electrostatic Repulsive Interaction	985 mA h g^{-1} at 0.25C 0.036 % for 1000 cycles	S-G 40 wt.%/1.1 mg cm^{-1}	S4
TiO_2/C	Electrospinning	Chemical adsorption	1238 mAh g^{-1} at 0.2C 0.13 % for 300 cycles	S/MWCNT 49 wt.%/3 mg cm^{-2}	S5
MWCNT	Self assembly	physicaly polysulfde-anchor	851 mAh g^{-1} at 0.5C 0.042 % for 100 cycles	Pure sulfur 80 wt.%/3 mg cm^{-2}	S6
Polypyrrole nanotube film(PYNF)	Vacuum fltration	Chemical adsorption	1102 mAh g^{-1} at 0.5C 0.11 % for 300 cycles	Ketjen Black/S 53 wt.%/3 mg cm^{-2}	S7
Carbonized sucrose-coated eggshell membranes (CSEMs)	Template method	physicaly polysulfde-anchor	1327 mAh g^{-1} at 0.1C 0.25 % for 100 cycles	CSEM/ Li_2S_6 3.2 mg cm^{-2}	S8
PAN-NC	Electrospinning	Chemical adsorption	1279 mAh g^{-1} at 0.2C 0.05 % for 100 cycles	Pure sulfur 60 wt.%/2.0 mg cm^{-2}	S9
Graphene-embedded carbon fiber (GFC)	Vacuum fltration	Chemical adsorption	1138 mAh g^{-1} at 1C 0.13 % for 300 cycles	Pure sulfur 60 wt.%/2.0 mg cm^{-2}	S10
FBN/G	Blading	Chemical adsorption	1100 mAh g^{-1} at 3C 0.0037 % for 1000 cycles	CNT/S 60 wt.%/1.5-3.0 mg cm^{-2}	S11
High-Flux Graphene Oxide	Blading	physicaly polysulfde-anchor	1182 mAh g^{-1} at 0.5C 0.29 % for 100 cycles	NPC/S 80 wt.%/ 1.2 mg cm^{-2}	S12
FMSiNP	Blading	Chemical adsorption and physicaly polysulfde-anchor	1294 mAh g^{-1} at 1.0C 0.038 % for 1500 cycles	CB/S 60 wt.%/ 1.2-1.6 mg cm^{-2}	This work

References

S1. Lu, Y.; Gu, S.; Guo, J.; Rui, K.; Chen, C.; Zhang, S.; Jin, J.; Yang, J.; Wen, Z., Sulfonic Groups Originated Dual-Functional Interlayer for High Performance Lithium-Sulfur Battery. ACS Appl Mater Interfaces 2017, 9 (17), 14878-14888.

S2. Singhal, R.; Chung, S.-H.; Manthiram, A.; Kalra, V., A free-standing carbon nanofiber interlayer for high-performance lithium–sulfur batteries. Journal of Materials Chemistry A 2015, 3 (8), 4530-4538.

S3. Yin, L.; Dou, H.; Wang, A.; Xu, G.; Nie, P.; Chang, Z.; Zhang, X., A functional interlayer as a polysulfides blocking layer for high-performance lithium–sulfur batteries. New Journal of Chemistry 2018, 42 (2), 1431-1436.

S4. Abbas, S. A.; Ibrahem, M. A.; Hu, L.-H.; Lin, C.-N.; Fang, J.; Boopathi, K. M.; Wang, P.-C.; Li, L.-J.; Chu, C.-W., Bifunctional separator as a polysulfide mediator for highly stable Li–S batteries. Journal of Materials Chemistry A 2016, 4 (24), 9661-9669.
S5. Zhao, T.; Ye, Y.; Lao, C. Y.; Divitini, G.; Coxon, P. R.; Peng, X.; He, X.; Kim, H. K.; Xi, K.; Ducati, C.; Chen, R.; Liu, Y.; Ramakrishna, S.; Kumar, R. V., A Praline-Like Flexible Interlayer with Highly Mounted Polysulfide Anchors for Lithium-Sulfur Batteries. Small 2017, 13 (40).
S6. Kim, H. M.; Hwang, J. Y.; Manthiram, A.; Sun, Y. K., High-Performance Lithium-Sulfur Batteries with a Self-Assembled Multiwall Carbon Nanotube Interlayer and a Robust Electrode-Electrolyte Interface. ACS Appl Mater Interfaces 2016, 8 (1), 983-7.
S7. Ma, G.; Wen, Z.; Wang, Q.; Shen, C.; Peng, P.; Jin, J.; Wu, X., Enhanced performance of lithium sulfur battery with self-assembly polypyrrole nanotube film as the functional interlayer. Journal of Power Sources 2015, 273, 511-516.
S8. Chung, S. H.; Manthiram, A., Carbonized eggshell membrane as a natural polysulfide reservoir for highly reversible Li-S batteries. Adv Mater 2014, 26 (9), 1360-5.
S9. Peng, Y.; Zhang, Y.; Wang, Y.; Shen, X.; Wang, F.; Li, H.; Hwang, B. J.; Zhao, J., Directly Coating a Multifunctional Interlayer on the Cathode via Electrospinning for Advanced Lithium-Sulfur Batteries. ACS Appl Mater Interfaces 2017, 9 (35), 29804-29811.
S10. Chai, L.; Wang, J.; Wang, H.; Zhang, L.; Yu, W.; Mai, L., Porous carbonized graphene-embedded fungus film as an interlayer for superior Li–S batteries. Nano Energy 2015, 17, 224-232.
S11. Fan, Y.; Yang, Z.; Hua, W.; Liu, D.; Tao, T.; Rahman, M. M.; Lei, W.; Huang, S.; Chen, Y., Functionalized Boron Nitride Nanosheets/Graphene Interlayer for Fast and Long-Life Lithium–Sulfur Batteries. Advanced Energy Materials 2017, 7 (13), 1602380.
S12. Shaibani, M.; Akbari, A.; Sheath, P.; Easton, C. D.; Banerjee, P. C.; Konstas, K.; Fakhfouri, A.; Barghamadi, M.; Musameh, M. M.; Best, A. S.; Ruther, T.; Mahon, P. J.; Hill, M. R.; Hollenkamp, A. F.; Majumder, M., Suppressed Polysulfide Crossover in Li-S Batteries through a High-Flux Graphene Oxide Membrane Supported on a Sulfur Cathode. ACS Nano 2016, 10 (8), 7768-79.